Food Innovation and Advances

ARTICLE

Open Access

https://doi.org/10.48130/fia-0024-0025

Food Innovation and Advances **2024**, 3(3): 268–278

Evaluation of cholesterol and cholates binding capacity and mechanism exploration of 'Yali' Pear polyphenol extracts: *in vitro*

Xu He[1#], Luyao Chen[1#], Yijing Pu[1], Jiankang Cao[1], Weibo Jiang[1*], Lingling Liu[2] and Chang Shu[3]

[1] *College of Food Science and Nutritional Engineering, China Agricultural University, Beijing 100083, PR China*
[2] *School of Environmental, Civil, Agricultural & Mechanical Engineering, University of Georgia, Athens, GA 30602, USA*
[3] *United States Department of Agriculture-Agricultural Research Service, Daniel K. Inouye US Pacific Basin Agricultural Research Center, 64 Nowelo Street, Hilo, HI 96720, USA*
[#] Authors contributed equally: Xu He, Luyao Chen
[*] Corresponding author, E-mail: jwb@cau.edu.cn

Abstract

In this study, three representative pears ('Yali' Pear, 'Huangguan' Pear, and 'Xuehua' Pear) peel/flesh polyphenol extracts were characterized by their antioxidant activity, polyphenol composition, and *in vitro* cholesterol/cholates binding capacity. 'Yali' Pear polyphenol extracts were selected to further investigate the mechanism of *in vitro* cholesterol/cholates lowering capacity. Lagergren adsorption kinetic and Freundlich isotherm models confirmed the occurrence of this combination. Turbidity, average particle size, transmission electron microscopy, and zeta potential combined confirmed the existence of some interaction between polyphenols and cholesterol/cholates. Cholesterol/cholates quenched the exogenous fluorescence of polyphenols by static mechanism. The thermodynamic interaction results revealed that the interaction between polyphenols and cholesterol is a spontaneous process, primarily driven by hydrogen bonding and hydrophobic interactions. Overall, this study aimed to investigate the confirmation of the binding removal properties of pear polyphenols on cholesterol/cholates to mitigate the adverse health effects of a high-fat diet.

Citation: He X, Chen L, Pu Y, Cao J, Jiang W, et al. 2024. Evaluation of cholesterol and cholates binding capacity and mechanism exploration of 'Yali' Pear polyphenol extracts: *in vitro*. *Food Innovation and Advances* 3(3): 268–278 https://doi.org/10.48130/fia-0024-0025

Introduction

The 21st century has witnessed dramatic changes in people's dietary structure and lifestyles. In particular, the widespread prevalence of Western-style diets and sedentary lifestyles has contributed to a continued surge in disorders of lipid metabolism, including obesity[1,2]. High levels of lipids and cholesterol in the blood are intimately correlated with lipid metabolism diseases[1]. The liver produces cholesterol, a sterol that also serves as a precursor to vitamin D, steroid hormones, and bile acid salts[3]. Through the movement of cholesterol micelles, the cholesterol consumed in food (animal food) is absorbed by the epithelial cells of the small intestine and reaches the liver and serum, where it acts as an essential part of the lipids that make up the lipid profile[4]. Based on earlier research, high cholesterol consumption is strongly correlated with cardiovascular disease, a serious threat to people's health[5,6]. However, given the negative side effects and high expense of cholesterol-lowering medications[7], researchers have come up with a novel idea: use naturally occurring active ingredients to adsorb and bind excess cholesterol in the gastrointestinal tract[3,4,6,8,9].

Bile acids, as products of cholesterol catabolism, facilitate the conversion of small intestinal cholesterol and lipids to fat. Following food intake, bile acids participate in the enterohepatic circulation and are stored in the gallbladder, which regulates cholesterol-level homeostasis[10]. When certain components of food bind to bile acid salts and are excreted from the body, the amount of bile acid salts stored in the gallbladder decreases, which encourages a greater flow of blood cholesterol to the liver and its conversion to bile acid salts[11]. Therefore, this pathway is also effectively reducing the blood cholesterol level[8,10,12]. Therefore, finding active adsorbents and assessing their ability to bind cholesterol and bile acid salts may be a promising new strategy for treating dyslipidemia in people.

Currently, pectin[4,13], dietary fiber[8,9,12], and other natural polysaccharides of cholesterol/bile salt adsorption capacity have been proved by numerous scholars. Polyphenols[14,15], as the principal active ingredients in fruits and vegetables, whose research related to the role of anti-obesity and blood lipid lowering *in vivo* and *in vitro* has sprung up[11,16–18]. Extracted condensed tannins (CTs) from banana peels were also discovered to aggregate with cholesterol/cholates[11]. Intake of CTs extract significantly promoted the excretion of bile acids in the feces of mice fed a high-fat diet and reduced the concentrations of liver lipids and plasma cholesterol. Similarly, apple condensed tannins have been proven to bind to cholesterol *in vitro*, which is supported by data from spectroscopic and morphological analyze[3]. Additionally, anthocyanins extracted from berries were shown to be effective in reducing cholesterol solubility in micelles and markedly reduced cholesterol uptake by Caco-2 cells in a concentration-dependent manner[18]. It was found that 1 mg/mL of berry extract was able to bind 20%–36% of sodium taurocholate.

Pears, as a fruit with high production and consumption, are also rich in phenolics in their peel and pulp, which have been endowed with a variety of health benefits, like antioxidant activity, blood pressure lowering, and lipid-lowering[19]. At

present, the exploration of pear activity is mostly concentrated on antioxidant and by-product utilization[20], with few reports focusing on the cholesterol/cholate binding effect of polyphenolic substances in pears. In the present study, anti-oxidant activity, polyphenol content composition and their correlation of three representative pears ('Yali' Pear, 'Huangguan' Pear, 'Xuehua' Pear) peel/pulp polyphenol extracts (PPEs) were compared. After comparatively analyzing PPEs' cholesterol/cholate binding capacity *in vitro* 'Yali' pear polyphenols (ARPPE, aRPPE) were elected for further study. Lagergren pseudo-primary and pseudo-secondary adsorption kinetic models were applied to discuss the process of binding cholesterol/cholate by PPEs. Besides, the adsorption mechanism of PPEs to cholesterol/cholates was investigated by combining Langmuir and Freundlich adsorption isotherm models. Crucially, the apparent mechanism of polyphenol binding to cholesterol/cholates was analyzed from the point of view of intermolecular interactions utilizing turbidimetry, zeta potential, and projected electron microscopy. Fluorescence analysis and thermodynamic interactions revealed possible binding forces between polyphenols and cholesterol/cholates. Overall, the goal of this study was to explore the binding and removing activities of fruit and vegetable polyphenols on cholesterol/cholates to alleviate the negative health impacts of high-fat diets.

Materials and methods

Materials

The peel and pulp of freshly picked 'Yali' Pears, 'Huangguan' Pears, and 'Xuehua' Pears (purchased froma fruit market, Beijing, China) were separated, and then frozen in liquid nitrogen and powdered and stored at −20 °C for further use.

Total polyphenol content (TPC), total flavonoid content (TFC)

TPC content

Referring to a previous method with minor modifications[21], 1.0 mL of the extraction, 1.0 mL of 10-fold diluted Folin-Ciocalteu reagent, and 3.0 mL of the 7.5% Na_2CO_3 solution were added and volumed with water to 10 mL. Then, the mixture was placed in a water bath at 70 °C for 1 h while keeping it out of the light, followed by an ice bath for 5 min, and the absorbance value was recorded at 760 nm. Gallic acid (0−150 μg/mL) was used as a reference standard to produce the standard curve. The results were expressed as gallic acid equivalent (mg GAE/100 g FW).

TFC content

0.5 mL of 2.2 medium supernatant was taken, 0.4 mL 5% $NaNO_2$ solution was added then shaken well and left to stand for 6 min, then 0.5 mL 10% $Al(NO_3)_3$ solution was added, this was then shaken and left to stand for 6 min, 4 mL 4% NaOH was then added and fixed with water to 10ml, shaken well and left to stand for 15 min. Absorbance was detected at 510 nm. With (0−300 μg/mL) catechin as the standard product, the standard curve was drawn, and the total flavonoid content was expressed by mg CAE/g FW, the calculation method was as outlined above.

Antioxidant activities

The DPPH free radical scavenging activity assay was based on a previous study[2]. The 3.0 mL of 100 μM DPPH solution (dissolved in ethanol) was mixed with 0.2 mL of diluted pear polyphenol supernatant and allowed to stand at room temperature for 60 min away from light. The absorbance at 517 nm was recorded and the results were expressed as Trolox equivalent (μmol TE/mg FW). Referring to a previous method, the reaction of 0.2 mL of sample solution with 3.0 mL of ABTS working solution was carried out for 10 min at room temperature, protected from light, and then the absorbance was recorded at 734 nm[22]. The results were expressed as Trolox equivalent (μmol TE/mg FW) for ABTS radical scavenging activity. Then, the antioxidant activity of PPEs was also evaluated using Fe^{3+} and Cu^{2+} reduction capacities, respectively[21]. The results were all expressed as Trolox equivalents (μmol TE/mg FW).

Finally, IBM SPSS Statistics 24 combined with Pearson's correlation coefficient were employed to analyze the correlation between the antioxidant activity of PPEs and their TPC, TFC.

Determination of cholesterol and cholate binding capacity *in vitro*

Cholesterol micelle solubility inhibition rate

Following a previous method[23], oleic acid, cholesterol, PBS buffer, sodium taurocholate, sodium chloride, and phosphatidylcholine were mixed and sonicated at 25 °C for 30−45 min to mix well, followed by incubation with constant temperature shaking at 37 °C for 24 h. Different concentrations of ARPPE and aRPPE solutions (buffer was used as a blank control) were added to the above micelles, mixed well, and then shaken at 37 °C for 2 h. The mixtures were then centrifuged at 10,000 r/min for 15 min (TGL 16C, Shanghai Anting Scientific Instrument Factory, Shanghai, China), and then analyzed by total cholesterol assay kit (Nanjing, China). Cholesterol concentration in the supernatant was determined using a total cholesterol assay kit (Nanjing Jiancheng Bioengineering Institute, Nanjing, China).

$$\text{Cholesterol micelle solubility inhibition rate (\%)} = \frac{C_0 - C}{C_0} \times 100\% \quad (1)$$

where, C_0 is the cholesterol concentration of the blank control; C is the cholesterol concentration after adding PPEs.

Cholesterol binding capacity

The PPEs solution (0−1 mg/mL) was mixed 1:1 (v/v) with 0.5 mg/mL of cholesterol solution (dissolved in 50 mM pH 7.4 Tris-HCl buffer), and the mixture was subsequently incubated at 37 °C for 2 h[13]. Additionally, the cholesterol-binding capacity under gastrointestinal conditions was briefly simulated: the pH of the above mixture was adjusted to 2.0 and 7.0 with 0.1 mol/L NaOH and 0.1 mol/L HCl. Next, after centrifugation at 10,000 r/min for 15 min, the supernatant was taken and the cholesterol content was determined according to the cholesterol kit operation. Cholesterol binding ability (CBA) was expressed as:

$$CBA = \frac{C_0 - C_1}{C_0} \times 100\% \quad (2)$$

where, C_0 is the cholesterol concentration of blank control, mmol/L; C_1 cholesterol concentration after adding PPEs, mmol/L.

The binding amount (Q) of PPEs to cholesterol is expressed as:

$$Q = \frac{(C_0 - C_1)V}{1000\,M} \quad (3)$$

where, Q is the binding quantity, mg/g; C_0 is the amount of cholesterol before binding, mg/L; C_1 is the amount of cholesterol after binding, mg/L; V, M are adsorption volume (L) and sample mass (g), respectively.

Cholate binding capacity

First, the 2 mmol/L sodium taurocholate (NaTC) and sodium glycylcholate (NaGC) reserves were prepared in PBS buffer and adjusted to the range considering that the concentration of bile acids in the human body is 1.5–7 mM[10,12]. The PPEs of 0–3 mg/mL were weighed to 2 mL each, respectively, to simply simulate the digestive environment of the gastrointestinal tract. To simulate the gastric environment, 3 mL of 10 mg/mL pepsin solution and 0.1 M HCl were added to adjust the pH to 2.0, and digestion was carried out in a thermostatic oscillatory incubator (120 rpm) at 37 °C for 1 h. Subsequently, to simulate the gastrointestinal environment, 4 mL of 10 mg/mL trypsin solution and 0.1 M NaOH were added to adjust the pH to 6.3, and digestion was carried out in a thermostatic oscillatory incubator at 37 °C. Then, 4 mL of 2 mM NaTC and NaGC were added to the digested PPEs solution, mixed well and incubated in a constant temperature incubator (120 rpm) for 1 h. After centrifugation at 8,000 rpm for 10 min, the supernatant was collected. One mL of the supernatant was mixed with 3 mL of 60 % (w/v) sulfuric acid solution, and the mixture was thoroughly mixed in a water bath at 70 °C for 20 min, then placed quickly in an ice bath for 5 min, and then cooled down to room temperature, the absorbance of the mixture was evaluated at 387 nm. A standard curve was established for determining the concentration of cholate, including a blank control. The cholate binding capacity (%) was expressed by calculating the difference in concentration of the system before and after the addition of PPEs. Similarly, the binding capacity of PPEs to NaTC and NaGC can be expressed by Eqn (3).

Kinetic model fitting

The Lagergren pseudo-primary (4) and pseudo-secondary models (5) were applied to analyze the kinetic processes involved in the binding of PPEs to cholesterol, NaTC, and NaGC[4,24].

$$q_t = q_e(1 - e^{-k_1 t}) \tag{4}$$

$$q_t = \frac{{q_e}^2 k_2 t}{1 + q_e k_2 t} \tag{5}$$

where, q_t (mg/g) represents the binding amount at t (h), q_e (mg/g) is the equilibrium adsorption capacity, k_1 (H^{-1}) and k_2 (g/mg·h) are the rate constants of Lagergren's pseudo-first-order and pseudo-second-order models, respectively.

Isothermal adsorption model fitting

Langmuir isotherm Eqn (6) and Freundlich isotherm adsorption Eqn (7) were used to fit the data to quantitatively evaluate the binding mechanism of PPEs on cholesterol, NaTC and NaGC[13,25].

$$\frac{1}{q_e} = \frac{1}{q_m} + \frac{1}{q_m K_L} \cdot \frac{1}{q_e} \tag{6}$$

$$ln_{q_e} = ln_{K_F} + \frac{1}{n} lnc_e \tag{7}$$

where, q_e: equilibrium adsorption capacity, mg/g; C_e: equilibrium concentration, mg/L; 1/n: adsorption index; K_L: Langmuir constant; K_F: Freundlich constant.

Mechanism investigation of pear polyphenol-cholesterol/cholate binding

Turbidity and Zeta-potentials

As previously reported[26], turbidity measurement was carried out using a UV-Vis spectrophotometer to detect absorbance at 600 nm. PPEs (0–2.5 mg/mL) and cholesterol/cholate (1 mg/mL) were combined 1:1 (v/v), and the reaction was shaken for 30 min at 25 °C before being measured. The formula for determining the turbidity of a complex in solution is turbidity = $A_{sample} - A_{buffer}$, where A is the sample's absorbance at 600 nm.

The charge-Zeta potential of the PPEs-cholesterol/cholic acid complex system was analyzed by Zetasizer Nano ZS instrument (Malvern Instruments, Malvern, U.K.). The composite system was formed by mixing PPEs (2.5 mg/mL) and cholesterol/cholate (0–5 mg/mL) at 25 °C at 1:1 (v/v) for 30 min.

DLS analysis

The particle size of the PPEs-cholesterol/cholates composite system was analyzed by dynamic light scattering (DLS) using a Zetasizer Nano ZS instrument (Malvern Instruments, Malvern, U.K.)[3]. Composite system: PPEs solution (2.0 mg/mL) and cholesterol and cholate solution (0–0.5 mg/mL) were mixed at 1:1 (v/v) for 30 min at 25 °C.

Transmission electron microscopy (TEM)

The apparent morphology of PPEs-cholesterol/cholate complexes was observed by TEM with reference to and slight modification of the method by Dolphen & Thiravetyan[27]. A solution of 3.0 mg/mL of PPEs was mixed with 1.0 mg/mL of cholesterol, NaTC, and NaGC 1:1 (v/v), respectively, and incubated at room temperature for 20 min. The PPEs and the mixture were added dropwise onto a carbon film on a 400-mesh copper grating, and then dried for 15 min before observation on the machine.

Fluorescence spectroscopy

The effects of cholesterol and cholate on the fluorescence spectra of PPEs solutions were determined with the addition of an exogenous fluorescent probe (1-PyCHO) using an F-4500 fluorescence spectrometer (Hitachi 4500, Tokyo, Japan)[11]. At room temperature, 2.0 mM of 1-PyCHO was mixed with 1.25 mg/mL of PPEs in a 3:1 (v/v) mixture for 20 min, and then different concentrations of cholesterol/cholates (0–2 mM) were mixed with the above mixture in a certain ratio, and the fluorescence spectra of the mixture were determined by centrifuging the supernatant at 8,000 rpm for 15 min after incubation at 37 °C for 60 min. The fluorescence spectrum of the mixture was determined by centrifugation at 8,000 rpm for 15 min. The excitation wavelength was set at 368 nm, and the widths of the emission and excitation slits were set at 5 nm, and the fluorescence spectra were collected at 350–600 nm.

The Stern-Volmer Eqn (8) was used to obtain the following fluorescence quenching parameters:

$$F_0/F = 1 + \mathrm{Ksv}\,[\mathrm{Q}] \tag{8}$$

Where F_0 and F denote the fluorescence intensity of the mixed system without and with PPEs; K_{sv} is the quenching constant ($K_{sv} = K_q \tau_0$), determined by linear regression of the curve of F_0/F vs [Q]; and [Q] is the concentration of the bursting agent.

The binding constant (K_a) and the number of binding sites (n) were calculated by the following equations:

$$\log\left[\frac{F_0 - F_1}{F_1}\right] = log K_a + n log\,[Q] \tag{9}$$

Analysis of thermodynamic effects

Referring to previous methods[2,28], thermodynamic parameters ΔH, ΔS, and ΔG were obtained based on the fluorescence spectral data at different temperatures (298.15, 303.15, and 310.15 K) upon Van't Hoff's Eqn (10) and the thermodynamic Eqn (11), which enabled us to determine the type of binding between duck pear polyphenols and cholesterol and cholates.

$$ln\frac{K_2}{K_1} = \left(\frac{1}{T_1} - \frac{1}{T_2}\right) \cdot \frac{\Delta H}{R} \quad (10)$$

$$\Delta G = \Delta H - T\Delta S = -RTlnK_a \quad (11)$$

Statistical analysis

All results are expressed as mean ± standard deviation. Statistical analysis was performed using IBM SPSS Statistics 24. Univariate analysis of variance (ANOVA) and Duncan test were used to analyze the significance of the data at $p < 0.05$.

Results and discussion

Analysis of TPC and TFC for PPEs

The total phenolic content (TPC) and total flavonoid content (TFC) of the peel and pulp of the three pear fruits were determined by ultrasound-assisted ethanol extraction (the extraction method is described in Supplemental File 1), and the results are displayed in Supplemental Table S1. The three types of pear peel that we studied had TPCs ranging from 457.49 to 591.33 mg GAE/100 g FW; the 'Huangguan' Pear enjoyed the highest TPC. In contrast, the TFC in the peel was 2-3 times greater than the TPC (1,132.08–1,307.08 mg GAE/100 g FW), with the 'Yali' Pear having the greatest TFC. Additionally, as presented in Supplemental Table S1, TPC and TFC detected in the peel of pears were remarkably high compared to the pulp, with similar results in fruits such as oriental pears[29], European pears[30], and apples. This is attributed to the propensity of polyphenols to accumulate in external tissues arising from their ability as plant secondary metabolites to resist invasion by pathogenic bacteria and to resist UV resistance[14]. A comparable study found TPC and TFC in ten different varieties of oriental pears. It found that all of the chemical constituents in the peel were approximately 6–20 times higher than those in the flesh[20]. In the present study, the total phenolic and flavonoid contents of pear peel and pulp were separately explored, which showed that the pear peel contained richer polyphenol components and contents, thus giving it higher biological activity.

Antioxidant activity of PPEs

CUPRAC, FRAP, DPPH, and ABTS were applied to comprehensively analyze the *in vitro* antioxidant activity of pear fruit polyphenol extracts. Among these four methods, ABTS and DPPH are based on a single electron transfer mechanism to determine the antioxidant capacity of the samples, while FRAP and CUPRAC utilize the redox properties of metal ions to determine the antioxidant capacity of the samples[2]. These four indexes had similar patterns in different varieties and different parts of the fruit, manifesting that the peel values were greater than the flesh (Supplemental Table S1). Correlation analyses were performed to analyze the contribution of TPC and TFC to the antioxidant capacity of the PPEs (Supplemental Table S2). Strong associations were observed between the TPC and TFC concentrations and all four antioxidant techniques (**, $p < 0.01$), indicating that phenolic chemicals are primarily responsible for the antioxidant potential of pears. It is worth noting that flavonoids are part of the phenolic group and may exert their antioxidant activity differently compared to other non-flavonoid phenols.

UPLC-MS analysis

Phenolic acids were identified as described in Supplemental File 1. As depicted in Supplemental Table S3, the main phenolics detected in pear skin were chlorogenic acid, arbutin, neochlorogenic acid, epigallocatechin, catechin, p-coumaric acid, transferulic acid, rutin, proanthocyanidin B_2, whereas chlorogenic acid and arbutin were predominant in the pulp. In line with the preceding total phenolic content and antioxidant activity, the kinds and concentrations of polyphenols in the peel were much greater than those in the pulp. More precisely, 'Huangguan' and 'Xuehua' Pears have higher levels of phenolic components, such as rutin and proanthocyanidin B_2, than 'Yali' Pear peel (ARPPE). However, the chlorogenic acid and arbutin contents of 'Yali' Pear were notably higher, especially the chlorogenic acid content, which reached 4.07 mg/g PPE. The polyphenolic profiles of 16 varieties of pear peels were confirmed that arbutin and chlorogenic acid were the dominant phenolic constituents in a previous study[30]. Chlorogenic acid has been shown to have anticancer, antiviral, and hypolipidemic effects, making it a promising chemopreventive agent[20]. Previous studies have also shown that antioxidant properties came from polyphenolic components[31].

Evaluation of cholesterol/cholate binding capacity of PPEs

Cholesterol/cholate binding capacity in vitro

In conjunction with the content of phenolic fractions in PPEs, five major phenolic monomers, chlorogenic acid, arbutin, neochlorogenic acid, epigallocatechin, and p-coumaric acid, were selected to assess their *in vitro* cholesterol and cholates binding *in vitro* ability. As illustrated in Supplemental Table S4, it was found that chlorogenic acid exhibited superior cholesterol and cholate binding abilities to the other components. Condensed from caffeic acid and quinic acid, chlorogenic acid has a more complicated structure and contains an ester link than the simple phenolic acids discussed previously[20]. A prior study stated that carboxyl esterification increased the affinity for proteins[32]. Another study noticed that the esterification of catechin gallate resulted in the formation of hydrophobic structural domains within the molecule[33]. These domains proved to possess more affinity for hydrophobic lipid bilayers compared to free catechins, making them more susceptible to hydrophobic binding to cholesterol and increasing cholesterol excretion.

The cholesterol and cholates binding capacity of the peel and pulp of the three pear fruits are displayed in Supplemental Fig. S1. PPEs showed better cholesterol binding capacity (20%–80%, Supplemental Fig. S1a) than the two cholate salts (5%–30%, Supplemental Fig. S1c, d), and 'Yali' Pear presented the optimal binding capacity, which was hypothesized to be possibly attributable to its highest chlorogenic acid content. Consequently, in the following study, 'Yali' Pear polyphenols will be the focus to probe the mechanism of their binding action with cholesterol/cholates.

The equilibrium adsorption capacity of ARPPE at pH 7.0 (240.79 ± 7.81 mg/g) was dramatically higher than that of pH

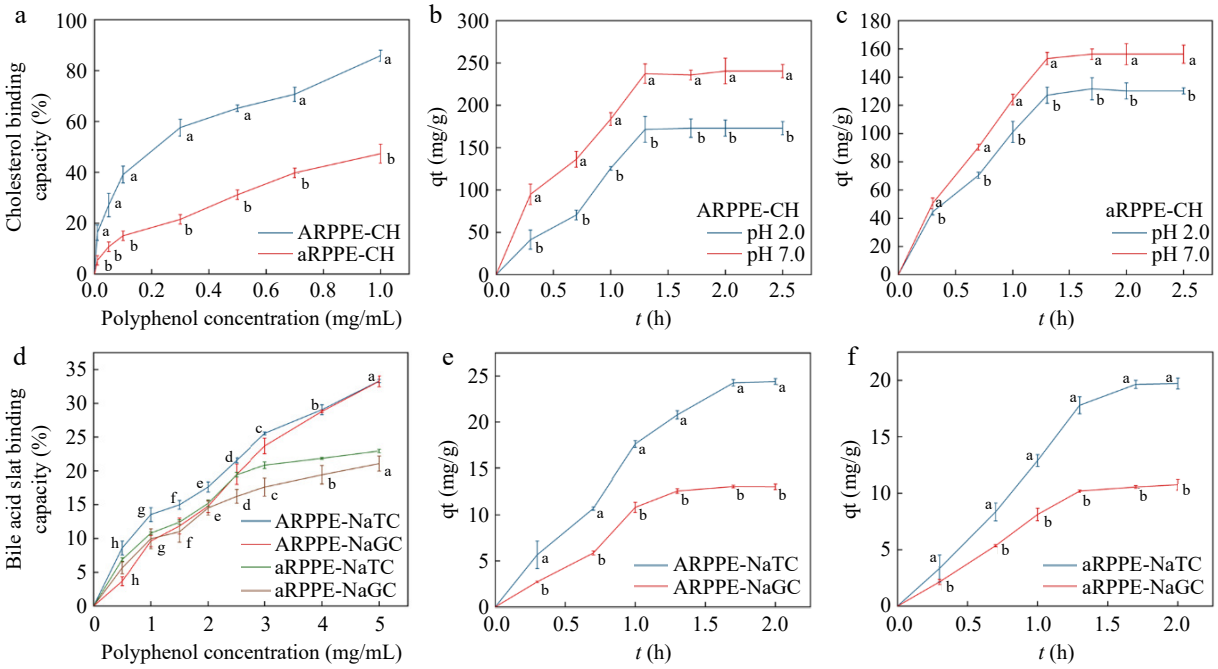

Fig. 1 Effect of ARPPE and aRPPE concentrations on their (a) cholesterol and (d) cholates binding; (b) and (c) are the equilibrium cholesterol binding of ARPPE and aRPPE at pH conditions simulating gastrointestinal digestion; (e) and (f) are the equilibrium binding of cholates.

2.0 (173.09 ± 6.34 mg/g) (Fig. 1a, b), with the same pattern also revealed for aRPPE. It indicated that PPEs may exhibit a more potent ability to reduce cholesterol concentration in the small intestine, and it was speculated that the weakly alkaline environment may promote the formation of complexes between polyphenols and cholesterol[6]. Consistent conclusions were also reached in a previous study[34]. Dietary fiber from bamboo shoots were also observed to incline to adsorb cholesterol in the small intestine[35]. It has been implicated that at pH 6.8, the trimethylamine group of phosphatidylcholine can interact with the galloyl group of EGCG in an ion-π-bonding interaction to form an EGCG-phosphatidylcholine complex, which reduces cholesterol solubility in micelles[36].

As for two cholates, ARPPE and aRPPE were able to attain more than 20% cholates binding at a concentration of 5 mg/mL (Fig. 1d) with a dose-dependent effect. Remarkably, PPEs bound to NaTC at a significantly higher rate than NaGC, implying that sulfonate groups have a superior adsorption capacity than amide groups. This difference in binding preference was explained by the higher polarity and dissociation of sulfonate groups relative to amide groups, which bound more readily. Likewise, banana condensed tannins[11] and grape seed polyphenols[16] have been demonstrated to have cholesterol and cholate-lowering effects, which contribute to the prevention of dyslipidemia and cardiovascular diseases.

Typically, dietary lipids are initially emulsified by cholates and lecithin in the small intestinal lumen and then enter micelles before being absorbed by small intestinal cells[37,38]. Therefore, declining the solubility of cholesterol in micelles is also an essential indicator for assessing cholesterol-lowering ability. As depicted in Supplemental Fig. S1b, the addition of PPEs solution to cholesterol micelles was able to reduce the solubility of cholesterol in the micelles with a dose effect. It illustrates that PPEs can form complexes by binding to cholesterol in the micelles to reduce the amount of cholesterol absorbed in the small intestine. Grape seed proanthocyanidins[16] and theaflavins[37] were identified to also markedly inhibit the formation of cholesterol micelles.

Adsorption kinetics

The adsorption of cholates primarily occurred within 90–100 min, while the adsorption of cholesterol largely took place within 80 min. After this point, the rate gradually decreased and reached a saturation point at equilibrium capacity Q_e (Fig. 2). It was found that the adsorption process of ARPPE and aRPPE for cholesterol and cholate were in agreement with both the pseudo-second-order adsorption kinetic model (chemisorption) and the pseudo-first-order adsorption kinetic model (physisorption), indicating that this process is complex, as evidenced by the correlation coefficients (R^2), which are all higher than 0.97. This mechanism, as described in Supplemental Table S5, was in line with a pseudo-second-order adsorption kinetic model, which postulates that chemical interactions regulate adsorption and that the concentrations of adsorbent and adsorbate are vital determinants of adsorption[24]. It was also discovered that the pseudo-second-order kinetic model (R^2: 0.96) better fits the adsorption of modified pectin to sodium cholate with support that the process is largely chemisorptive[4]. Interestingly, the present study detected that the pseudo-first-order kinetic model also fitted the adsorption process of cholesterol and cholate better (higher correlation coefficients and equilibrium adsorption capacity), which suggests that physical and chemical adsorption may coexist[39]. It has been proposed that physical and chemical adsorption are two fundamentally different forms of adsorption, but they can occur simultaneously on the same surface. There was an indication that ion-ion interactions between the nonpolar molecules cholesterol and cholates and small molecules chemisorb them onto pectin/lignocellulose nanofibers/chitin nanofibers bionanocomposite, while van der Waals bonding physically adsorbs cholesterol molecules onto the

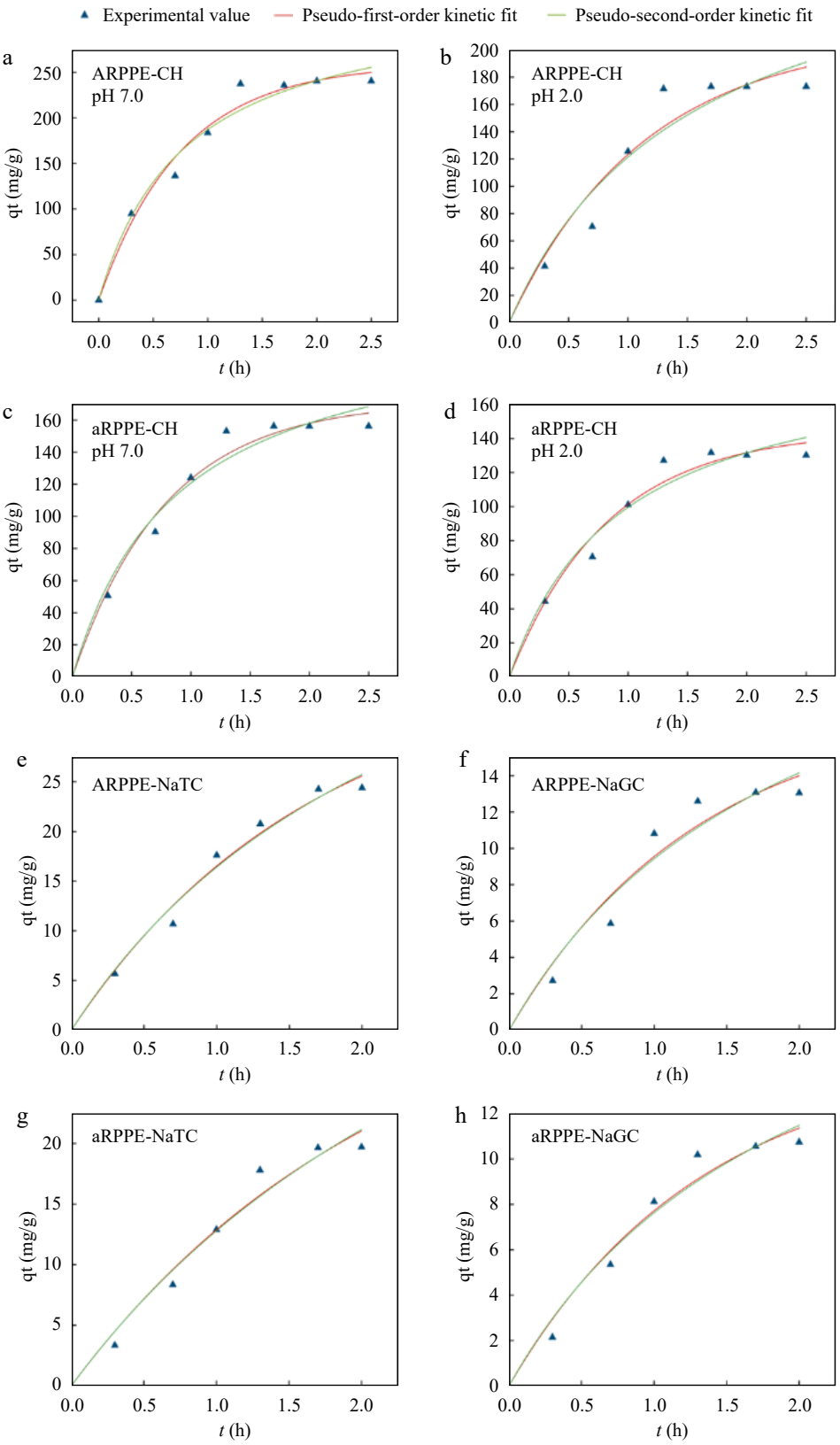

Fig. 2 Binding kinetic models of ARPPE and aRPPE for cholesterol and cholates-Lagergren pseudo-first-order and pseudo-second-order fits. (a), (b) Kinetic fits of ARPPE for cholesterol binding ability at pH 7.0 and pH 2.0, respectively; (c), (d) kinetic fits of aRPPE for cholesterol binding ability at pH 7.0 and pH 2.0, respectively; (e), (f) kinetic fits of ARPPE for the binding ability of sodium taurocholate and sodium glycyl cholate, respectively; (g), (h) kinetic fits of aRPPE for the binding ability of sodium taurocholate and sodium glycyl cholate, respectively.

adsorbent[13]. Furthermore, for cholesterol adsorption fitting, the theoretical Q_e at pH 7.0 was observed to be greater than that at pH 2.0, which is consistent with the findings above that PPEs preferred to adsorb cholesterol in the small intestine.

Isothermal adsorption modeling

Additional examination of the cholesterol and cholates adsorption isotherms on PPEs was performed (Fig. 3, Supplemental Table S6). The Langmuir model quantitatively assumes the formation of a monolayer of adsorbates on the outer surface of the adsorbent without further adsorption[4]. The Freundlich model, on the other hand, specifies the adsorption properties of a non-homogeneous surface[13,24]. Despite the good fit of both isotherm models (high correlation coefficients), the Freundlich isotherm model confirmed that adsorption can occur on non-homogeneous surfaces according to R^2 and Q_m. The distribution of surface functional groups and the size of the surface pore shape may be related to this[25]. Nonetheless, the data for the equilibrium capacity Qe are in better agreement with the Langmuir isotherm, pointing to a homogeneous structure of the adsorbent[4]. Similar results were also observed by a previous study[13,25].

Exploration of polyphenol-cholesterol/cholate binding mechanisms

Turbidity, DLS analysis, TEM

Turbidity, mean particle size, and TEM were initially employed to analyze the binding of PPEs to cholesterol (CH), sodium taurocholate (NaTC), and sodium glycylcholate (NaGC). The turbidity of the PPEs complexes all climbed considerably as the PPEs concentration increased, as seen in Fig. 4a–c, perhaps indicating the production of bigger binders[11]. Figure 4d–f depicts the average particle sizes of the complexes follow the addition of CH, NaTC, and NaGC. Following the addition of 0.5 mg/mL cholesterol, the ARPPE-CH complex's particle size grew from 635.15 to 805.11 nm, while the particle sizes of the other complexes increased to differing degrees. Consistent conclusions were also discovered on the effect of banana-condensed tannins and apple-condensed tannins on cholesterol using DLS particle size analysis[3,38]. Meanwhile, the addition of CH/NaTC/NaGC aggregated the solution particles and changed their size, as illustrated by the TEM picture (Fig. 4j). This is consistent with the earlier findings and indicates that cholesterol and/or cholates can interact with certain PPE components through aggregation. Theaflavins exhibited the same behavior[37]. All the above structures elucidated the ability of PPEs to aggregate with cholesterol and bile salts, which in turn reduces the digestion and absorption of lipids.

Zeta-potential

The potential between suspended solid particles and the liquid phase is frequently measured using zeta potential. Generally, a rise in the zeta-potential's absolute value indicates that the stability of the aggregates generated in the solution has improved[11,26]. The PPEs solutions' initial zeta potential values, depicted in Fig. 4g–i, were negative, which was

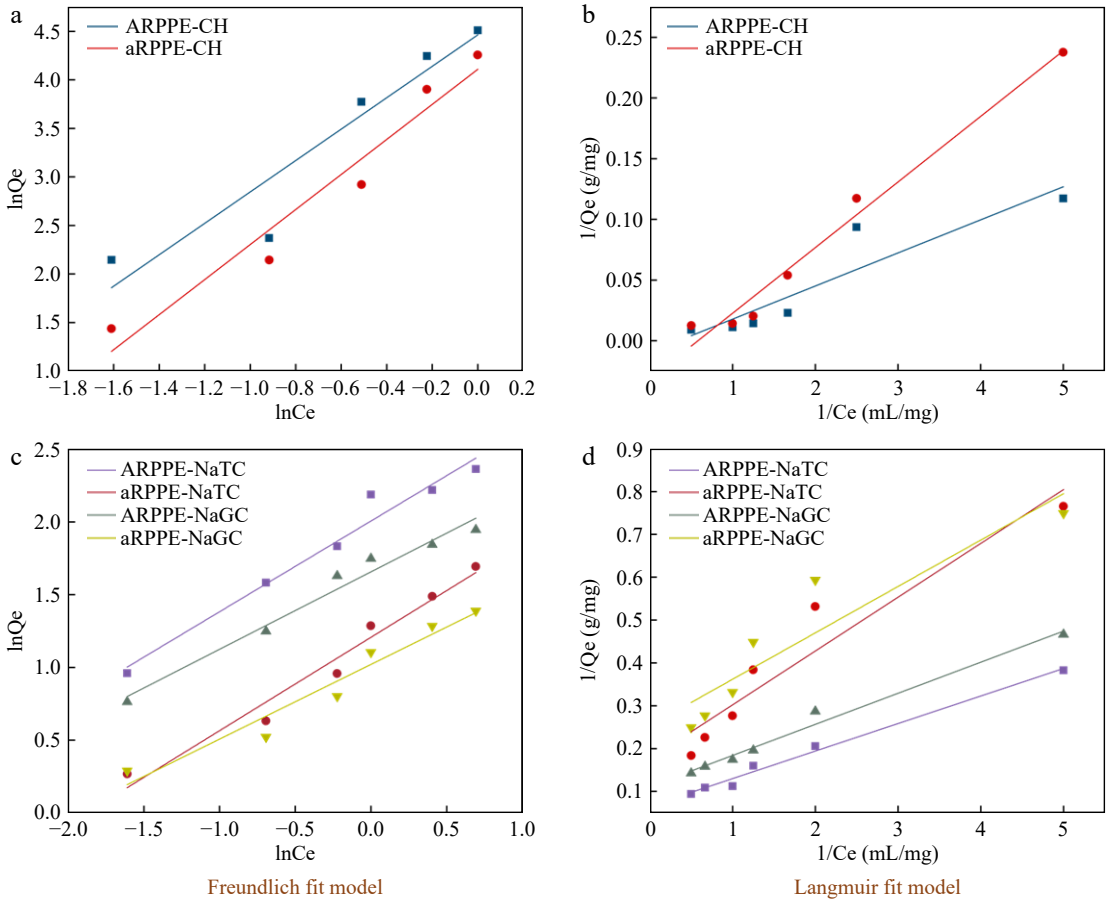

Fig. 3 Isothermal adsorption modelling of cholesterol and cholates by ARPPE and aRPPE-Freundlich, Langmuir fitting. Where (a) and (b) are cholesterol; (c) and (d) are cholates.

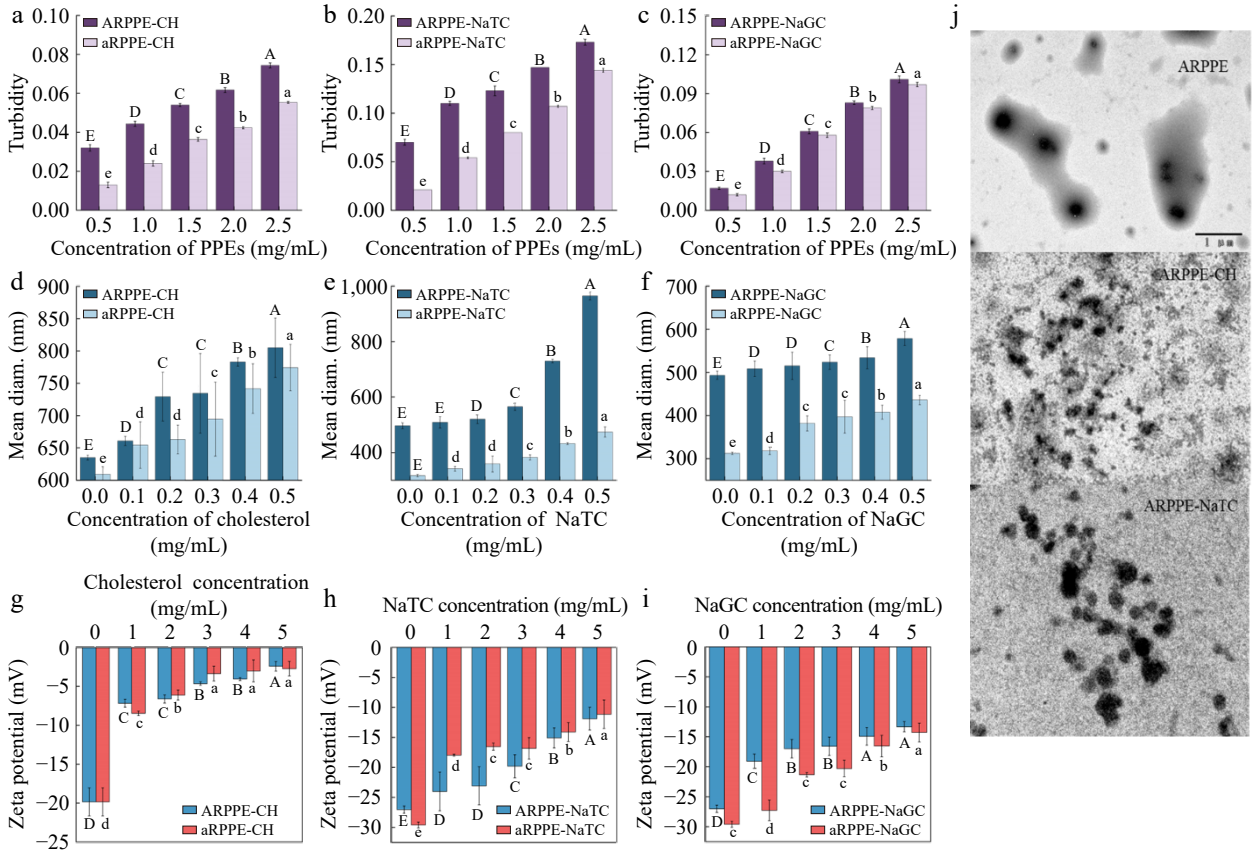

Fig. 4 Analysis of the mechanism of action of PPEs binding to cholesterol and cholates. (a)–(c) are turbidity, (d)–(f) are DLS analysis, (g)–(i) are zeta-potentials, and (j) is TEM.

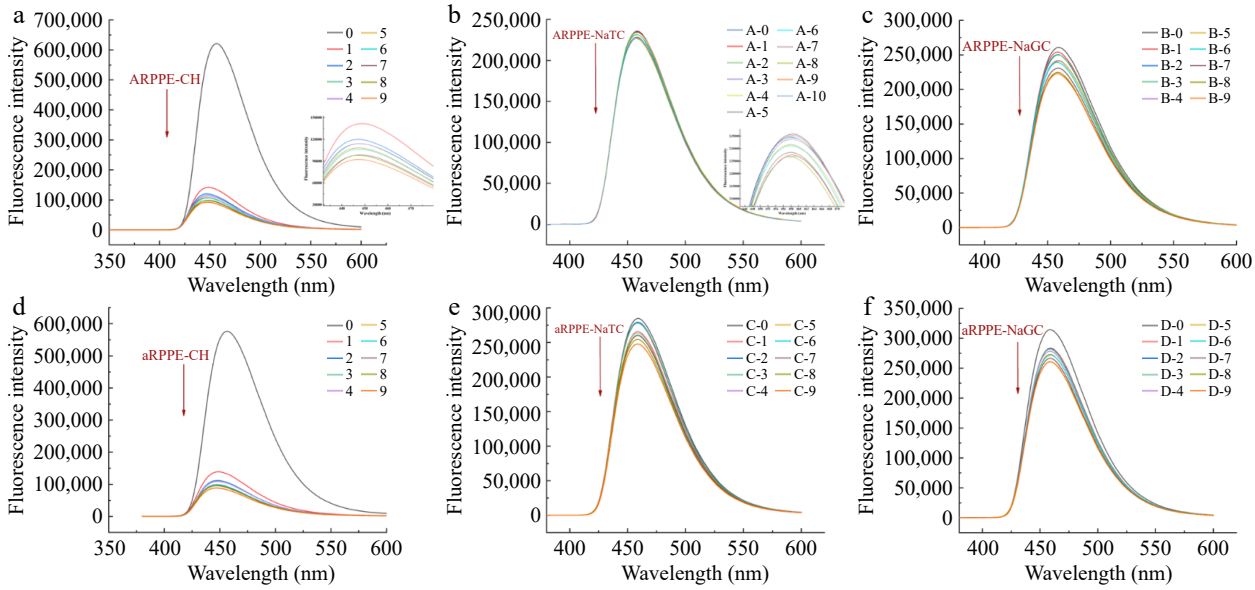

Fig. 5 Exogenous fluorescence spectra of different concentrations of PPEs bound to cholesterol (CH), sodium taurocholate (NaTC), and sodium glycinate cholate (NaGC) at 310 K.

explained by their negative charge in the aqueous solution. With the addition of cholesterol and cholates, the absolute value of the zeta potential of the mixture decreased dramatically ($p < 0.05$), signifying a reduction in the stability of the mixture solution. The higher the cholesterol/cholates concentration, the lower the stability of the mixture. It indicated some kind of binding interaction between ARPPE, aRPPE and cholesterol/cholates molecules, which produced effects similar to electrostatic interactions, like electrostatic repulsion[38]. It was noticed that condensed tannins could substantially decrease the pancreatic lipase solution's zeta potential's absolute value, and they traced this to electrostatic shielding[26].

Fluorescence spectroscopy analysis

Recently, studies using fluorescence spectroscopy to analyze intermolecular interactions have mushroomed[2,26,28,32]. For substances that are not fluorescent, we investigated the interaction between PPEs and cholesterol by fluorescence spectroscopy of an exogenous fluorescent probe (1-pyrenecarboxaldehyde)[11]. The ARPPE/aRPPE-1-pyrenecarboxaldehyde complex's fluorescence intensity decreased and fluorescence quenching took place as a result of adding cholesterol solution (Fig. 5a, d). The mixture's fluorescence intensity gradually decreased as the concentration of cholesterol increased, and a slight blue shift (from 460 to 450 nm) was seen in the maximum emission wavelength. This implied that ARPPE, aRPPE, and cholesterol interacted to form a new complex, and the blue shift phenomenon indicated that the polarity of the microenvironment surrounding the PPEs' cholesterol decreased. This is also consistent with the idea that cholesterol may change the polarity of an environment by binding to hydrophobic groups in polyphenols.

Further calculations using the Stern-Volmer equation yielded the fluorescence burst constant K_{sv}, the binding constant K_a and the binding site n (Supplemental Table S7). The binding constants reflected the binding affinity of the PPEs for cholesterol, which showed that the affinity of ARPPE for cholesterol was higher than that of aRPPE, which could be attributed to the role of the more abundant polyphenol fraction in the former. A fluorescence burst was also observed in the PPEs-pyrene carboxaldehyde-cholate complexes (Fig. 5b, c, e & f). As evidenced by the binding constants of PPEs to the two bound cholate salts, the binding constant of PPEs to NaTC (0.2447) was higher than that of NaGC (0.1307), which accounted for the fact that sulfonate groups are more polar than amide groups and are more likely to be bound. It is in accordance with the previous finding that pear polyphenols have higher binding to NaTC than NaGC.

Exploration of thermodynamic effects

The majority of the non-covalent interactions that polyphenols exploit to attach to proteins and other molecules to form complexes include hydrogen bonding, van der Waals forces, hydrophobic interactions, and electrostatic interactions[40]. Specifically, thermodynamic interaction analysis may be conducted to determine the potential forms of binding between PPEs and the cholesterol and cholates. The cholesterol and ARPPE/aRPPE interaction showed negative enthalpy change values (−47.8650, −35.1180 kJ/mol, respectively), reflecting an exothermic reaction mechanism (Supplemental Table S8). The primary contact force between cholesterol and 'Yali' Pear polyphenol is non-covalent, as evidenced by the failure to attain the requisite enthalpy change value (200−400 kJ/mol) due to the low enthalpy change value[11]. Furthermore, the fact that $\Delta G < 0$ for this reaction points to that the PPEs are naturally occurring complexes with cholesterol, and the fact that $\Delta H < 0$ and $\Delta S > 0$ for the interaction of ARPPE/aRPPE with cholesterol suggests that these interactions are primarily driven by entropy and enthalpy[11,28,41], with hydrogen bonding and hydrophobic interactions acting as the chief driving force. These outcomes are in concordance with those obtained by fluorescence spectroscopy analysis. Taken together, the hydrophobic interactions between the PPEs molecules and the cholesterol, as well as the formation of hydrogen bonds between the two, are exothermic processes.

When it comes to cholates, the reaction's $\Delta G < 0$ value suggests that the PPEs are complexes that spontaneously form with NaTC and NaGC as well. In contrast to cholesterol, the process is a heat-absorbing reaction. Furthermore, both the ΔH and ΔS of these reaction processes were larger than 0, implying that hydrophobic interactions dominate the binding process between PPEs and NaTC/NaGC, which is a spontaneous reaction triggered by entropy change[41]. It is known that PPEs contain hydrophobic aromatic nuclei with multiple phenolic hydroxyl groups, whereas the hydrophobic groups of cholates are located on a convex surface. Hence, the way that PPEs and cholates interact may be influenced by hydrophobic interactions. In a comparable manner, isothermal titration calorimetry research demonstrated that hydrophobic interactions and hydrogen bonds are essential to binding banana condensed tannins to bile salts[11].

Conclusions

In this study, 'Yali' Pear polyphenols (ARPPE, aRPPE) with the highest content of chlorogenic acid exhibited optimal *in vitro* cholesterol/cholates binding capacity. The adsorption of cholesterol/cholates by ARPPE and aRPPE was well fitted by both the Lagergren pseudo-first-order kinetic model and the pseudo-second-order kinetic model, suggesting that the process is complex, with both physical and chemical adsorption. Additionally, the Freundlich isotherm model validates that this adsorption process can take place on a non-homogeneous surface, which may be related to the size of the surface pore shape and the distribution of surface functional groups.

The mean particle size of PPEs increased considerably with the incorporation of CH, NaTC, and NaGC, and the TEM results also revealed that aggregation occurred between them. Also, the dramatic decrease in the absolute value of the complexes' zeta potential confirmed this intermolecular binding interaction, which may produce an effect similar to electrostatic interactions. It was also discovered that cholesterol/cholates quenched the exogenous fluorescence of ARPPE, aRPPE through a static mechanism, and the thermodynamic interaction results indicated that the interaction between 'Yali' pear polyphenols and cholesterol is a spontaneous process, mainly driven by hydrogen bonding, and hydrophobic interactions. In sum, the present research confirms that pear polyphenols contribute to mitigating the digestion and absorption of lipids and offer health benefits by interacting with cholesterol and cholates.

Pear peel and pulp polyphenol extraction

0.1% hydrochloric acid was added to avoid polyphenoloxidation when the freeze-dried powder of pear peel and pulp (10 g) was extracted with 60% ethanol at a ratio of 1:10 (w/v) for 30 min at 50 °C. After centrifugation, the supernatant was recovered, and using the technique described above, the bottom layer of the residue was extracted three times. After centrifugation, the supernatants were combined and freeze-dried after rotary evaporation to remove ethanol to obtain pear polyphenol extracts (PPEs). The PPEs included: 'Yali' Pear peelpolyphenol extract-ARPPE, 'Yali' Pear pulp-aRPPE; 'Huangguan' Pear peel polyphenol extract-BRPPE, 'Huangguan' Pear pulp-bRPPE; 'Xuehua' Pear peel polyphenol extract-CRPPE,'Xuehua' Pear pulp-cRPPE.

UPLC-MS analysis of pear polyphenol extracts (PPEs)

Preparation of the sample to be tested: 2 g of PPE slyophilized powder was taken, 5.0 mL of 0.1% hydrochloric acid-methanol (v/v) solvent was added, and the air bubbles were removed by sonication and then stored over 0.22 μm forreserve. ACQUITY UPLC I Class ultra-performance liquid chromatography (UPLC Water TM, USA) and tandem Thermo Q Exactive Focus high-resolution mass spectrometer (ThermoScientific, Waltham, MA, USA) were used for the identification and quantification of pear polyphenols. The major polyphenolsin PPEs were identified and quantified by comparing the retention times and peak areas with those of the corresponding standards. Xcalibur software (Thermo Scientific) was used for data acquisition and analysis of the liquid chromatography tandem mass spectrometry system. Specific methods are described in the Supplementary Material.

Author contributions

The authors confirm contributions to the paper as follows: study conception and design: He X, Jiang W; data collection: Chen L, Pu Y, Cao J; analysis and interpretation of results: He X, Chen L; draft manuscript preparation: He X, Chen L. All authors reviewed the results and approved the final version of the manuscript.

Data availability

All data generated or analyzed during this study are included in this published article and its supplementary information files.

Acknowledgments

This work was supported by the National Natural Science Foundation of China (No. 32172270).

Conflict of interest

The authors declare that they have no conflict of interest.

Supplementary Information accompanies this paper at (https://www.maxapress.com/article/doi/10.48130/fia-0024-0025)

Dates

Received 7 May 2024; Revised 16 July 2024; Accepted 20 July 2024; Published online 14 August 2024

References

1. He X, Chen L, Pu Y, Wang H, Cao J, et al. 2023. Fruit and vegetable polyphenols as natural bioactive inhibitors of pancreatic lipase and cholesterol esterase: Inhibition mechanisms, polyphenol influences, application challenges. *Food Bioscience* 55:103054
2. Huang R, Zhang Y, Shen S, Zhi Z, Cheng H, et al. 2020. Antioxidant and pancreatic lipase inhibitory effects of flavonoids from different citrus peel extracts: an *in vitro* study. *Food Chemistry* 326:126785
3. Zeng X, Du Z, Ding X, Jiang W. 2020. Characterization of the direct interaction between apple condensed tannins and cholesterol in vitro. *Food Chemistry* 309:125762
4. Chen L, He X, Pu Y, Wang H, Cao J, et al. 2024. Adsorption removal properties of β-cyclodextrin-modified pectin on cholesterol and sodium cholate. *Food Chemistry* 430:137059
5. Li X, Jiang H, Pu Y, Cao J, Jiang W. 2019. Inhibitory Effect of Condensed Tannins from Banana Pulp on Cholesterol Esterase and Mechanisms of Interaction. *Journal of Agricultural and Food Chemistry* 67(51):14066−73
6. Chen L, He X, Pu Y, Cao J, Jiang W. 2023. Polysaccharide-based biosorbents for cholesterol and bile salts in gastric-intestinal passage: Advances and future trends. *Comprehensive Reviews in Food Science and Food Safety* 22(5):3790−813
7. Paraskevas KI, Gloviczki P, Antignani PL, Comerota AJ, Dardik A, et al. 2022. Benefits and drawbacks of statins and non-statin lipid lowering agents in carotid artery disease. *Progress in Cardiovascular Diseases* 73:41−47
8. Zheng Y, Xu B, Shi P, Tian H, Li Y, et al. 2022. The influences of acetylation, hydroxypropylation, enzymatic hydrolysis and cross-linking on improved adsorption capacities and *in vitro* hypoglycemic properties of millet bran dietary fibre. *Food Chemistry* 368:130883
9. Zhu WW, Zhang Y, Tang CH. 2023. Maximizing cholesterol-lowering benefits of soy protein isolate by glycation with soy soluble polysaccharide. *Food Hydrocolloids* 135:108131
10. Yoshie-Stark Y, Wäsche A. 2004. In vitro binding of bile acids by lupin protein isolates and their hydrolysates. *Food Chemistry* 88(2):179−84
11. Li X, Jiao W, Zhang W, Xu Y, Cao J, et al. 2019. Characterizing the interactions of dietary condensed tannins with bile salts. *Journal of Agricultural and Food Chemistry* 67(34):9543−50
12. Huang YL, Ma YS, Tsai YH, Chang SKC. 2019. *In vitro* hypoglycemic, cholesterol-lowering and fermentation capacities of fiber-rich orange pomace as affected by extrusion. *International Journal of Biological Macromolecules* 124:796−801
13. Khorasani AC, Kouhfar F, Shojaosadati SA. 2021. Pectin/lignocellulose nanofibers/chitin nanofibers bionanocomposite as an efficient biosorbent of cholesterol and bile salts. *Carbohydrate Polymers* 261:117883
14. Chen L, Pu Y, Xu Y, He X, Cao J, et al. 2022. Anti-diabetic and anti-obesity: Efficacy evaluation and exploitation of polyphenols in fruits and vegetables. *Food Research International* 157:111202
15. He X, Pu Y, Chen L, Jiang H, Xu Y, et al. 2023. A comprehensive review of intelligent packaging for fruits and vegetables: Target responders, classification, applications, and future challenges. *Comprehensive Reviews in Food Science and Food Safety* 22(2):842−81
16. Ngamukote S, Mäkynen K, Thilawech T, Adisakwattana S. 2011. Cholesterol-lowering activity of the major polyphenols in grape seed. *Molecules* 16(6):5054−61
17. Padilla-Camberos E, Flores-Fernandez JM, Fernandez-Flores O, Gutierrez-Mercado Y, Carmona-de la Luz J, et al. 2015. Hypocholesterolemic effect and *in vitro* pancreatic lipase inhibitory activity of an opuntia ficus-indica extract. *BioMed Research International* 2015:e837452
18. Chamnansilpa N, Aksornchu P, Adisakwattana S, Thilavech T, Mäkynen K, et al. 2020. Anthocyanin-rich fraction from Thai berries interferes with the key steps of lipid digestion and cholesterol absorption. *Heliyon* 6(11):e05408
19. Galvis Sánchez AC, Gil-lzquierdo A, Gil MI. 2003. Comparative study of six pear cultivars in terms of their phenolic and vitamin C contents and antioxidant capacity. *Journal of the Science of Food and Agriculture* 83(10):995−1003
20. Li X, Wang T, Zhou B, Gao W, Cao J, et al. 2014. Chemical composition and antioxidant and anti-inflammatory potential of peels and flesh from 10 different pear varieties (*Pyrus* spp.). *Food Chemistry* 152:531−38
21. Wang H, Zhang Y, Pu Y, Chen L, He X, et al. 2023. Composite coating of guar gum with salicylic acid alleviates the quality deterioration of vibration damage in 'Huangguan' pear fruit through the regulation of antioxidant metabolism. *Postharvest Biology and Technology* 205:112476

22. Jiménez-Aspee F, Theoduloz C, Gómez-Alonso S, Hermosín-Gutiérrez I, Reyes M, et al. 2018. Polyphenolic profile and antioxidant activity of meristem and leaves from "chagual" (*Puya chilensis* Mol.), a salad from central Chile. *Food Research International* 114:90−96
23. Zhang HL, Wu QX, Wei X, Qin XM. 2020. Pancreatic lipase and cholesterol esterase inhibitory effect of *Camellia nitidissima* Chi flower extracts *in vitro* and *in vivo*. *Food Bioscience* 37:100682
24. Kartal F, Denizli A. 2020. Molecularly imprinted cryogel beads for cholesterol removal from milk samples. *Colloids and Surfaces B: Biointerfaces* 190:110860
25. Shariful MI, Sharif SB, Lee JJL, Habiba U, Ang BC, et al. 2017. Adsorption of divalent heavy metal ion by mesoporous-high surface area chitosan/poly (ethylene oxide) nanofibrous membrane. *Carbohydrate Polymers* 157:57−64
26. Pu Y, Chen L, He X, Cao J, Jiang W. 2023. Soluble polysaccharides decrease inhibitory activity of banana condensed tannins against porcine pancreatic lipase. *Food Chemistry* 418:136013
27. Dolphen R, Thiravetyan P. 2011. Adsorption of melanoidins by chitin nanofibers. *Chemical Engineering Journal* 166(3):890−95
28. Li S, Hu X, Pan J, Gong D, Zhang G. 2021. Mechanistic insights into the inhibition of pancreatic lipase by apigenin: Inhibitory interaction, conformational change and molecular docking studies. *Journal of Molecular Liquids* 335:116505
29. Cui T, Nakamura K, Ma L, Li JZ, Kayahara H. 2005. Analyses of Arbutin and Chlorogenic Acid, the Major Phenolic Constituents in Oriental Pear. *Journal of Agricultural and Food Chemistry* 53(10):3882−87
30. Lin LZ, Harnly JM. 2008. Phenolic Compounds and Chromatographic Profiles of Pear Skins *(Pyrus* spp.). *Journal of Agricultural and Food Chemistry* 56(19):9094−101
31. Oluwajuyitan TD, Ijarotimi OS, Fagbemi TN. 2022. Plantain-based dough meal: Nutritional property, antioxidant activity and dyslipidemia ameliorating potential in high-fat-induced rats. *Food Frontiers* 3(3):489−504
32. Tang B, Huang Y, Ma X, Liao X, Wang Q, et al. 2016. Multispectroscopic and docking studies on the binding of chlorogenic acid isomers to human serum albumin: Effects of esteryl position on affinity. *Food Chemistry* 212:434−42
33. Ikeda I, Kobayashi M, Hamada T, Tsuda K, Goto H, et al. 2003. Heat-epimerized tea catechins rich in gallocatechin gallate and catechin gallate are more effective to inhibit cholesterol absorption than tea catechins rich in epigallocatechin gallate and epicatechin gallate. *Journal of Agricultural and Food Chemistry* 51(25):7303−7
34. Luo X, Wang Q, Zheng B, Lin L, Chen B, et al. 2017. Hydration properties and binding capacities of dietary fibers from bamboo shoot shell and its hypolipidemic effects in mice. *Food and Chemical Toxicology* 109:1003−9
35. Wu W, Hu J, Gao H, Chen H, Fang X, Mu H, et al. 2020. The potential cholesterol-lowering and prebiotic effects of bamboo shoot dietary fibers and their structural characteristics. *Food Chemistry* 332:127372
36. Kobayashi M, Nishizawa M, Inoue N, Hosoya T, Yoshida M, et al. 2016. Epigallocatechin gallate decreases the micellar solubility of cholesterol via specific interaction with phosphatidylcholine. *Journal of Agricultural and Food Chemistry* 62(13):2881−90
37. Vermeer MA, Mulder TPJ, Molhuizen HOF. 2008. Theaflavins from black tea, especially theaflavin-3-gallate, reduce the incorporation of cholesterol into mixed micelles. *Journal of Agricultural and Food Chemistry* 56(24):12031−36
38. Li X, Pu Y, Xu Y, Cao J, Jiang W. 2021. Potential hypolipidemic effects of banana condensed tannins through the interaction with digestive juice components related to lipid digestion. *Journal of Agricultural and Food Chemistry* 69(31):8703−13
39. Vareda JP. 2023. On validity, physical meaning, mechanism insights and regression of adsorption kinetic models. *Journal of Molecular Liquids* 376:121416
40. Guo Q, Xiao X, Lu L, Ai L, Xu M, et al. 2022. Polyphenol–Polysaccharide Complex: Preparation, Characterization, and Potential Utilization in Food and Health. *Annual Review of Food Science and Technology* 13(1):59−87
41. Caruso ÍP, Filho JMB, de Araújo AS, de Souza FP, Fossey MA, et al. 2016. An integrated approach with experimental and computational tools outlining the cooperative binding between 2-phenylchromone and human serum albumin. *Food Chemistry* 196:935−42